

Plasmonic energy transfer through local excitations in nanoparticle waveguides.

Raúl A. Bustos-Marín^{1,2}, Eduardo A. Coronado² and Horacio M. Pastawski¹

¹*Instituto de Física Enrique Gaviola and Facultad de Matemática, Astronomía y Física, Universidad Nacional de Córdoba, Ciudad Universitaria, 5000 Córdoba, Argentina. and*

²*INFIQC, Departamento de Fisicoquímica, Facultad Ciencias Químicas, Universidad Nacional de Córdoba, Ciudad Universitaria, 5000 Córdoba, Argentina.*

(Date text)

We study the critical conditions for plasmonic energy transfer from a locally excited nanoparticle (LE-NP) to a linear array of small NPs. By obtaining the analytical excitation spectra we distinguish different propagation regimes. Besides the expected transfer controlled by resonant and localized states, we find a regime of virtual states that plays a central role in excitation transfer. Contrary to common wisdom, optimal energy transfer does not occur for an homogeneous configuration, i.e. when the LE-NP is indistinguishable from the NPs along the waveguide. Instead, the highest excitation transfer occurs at the virtual to localized state transition. The extreme sensitivity of this transition to the system parameters enables new designs for plasmonic applications.

Electromagnetic energy can be focused and guided below the light diffraction limit by transforming it into surface plasmon polaritons that can propagate as a collective excitation along one dimensional arrays of nanoparticles (NPs).[1] This feature has attracted significant attention due to its potential applications in optoelectronic devices such as sub-wavelength waveguides, random lasers, optical traps, and hot-spot based plasmonic sensors for ultra-sensitive spectroscopy [1–3]. Although previous works have already addressed the question of how to achieve a high degree of localization of plasmonic excitation [4] or have studied the plasmon propagation on ordered NP chains [2, 5], a fundamental question remains open: how to transform this localized excitation into a propagating signal. This poses a big challenge for both experiments and theory since there is a broad range of parameters that one should explore before achieving an optimal tailoring of the plasmonic excitation transfer. In this work we use a general formalism capable of giving a universal description of the excitation dynamics. We find a wealth of propagation regimes mediated by *localized*, *virtual* and *resonant* states, not described so far in this context. Quite suprisingly, we prove that the virtual to localized states transition provides a route to optimal excitation transfer.

The systems under consideration is described in Fig. 1. It consists of a linear array of metal NPs coupled to a locally excited (LE) NP. This situation leads to the usual coupled dipole approximation [2, 5–7], where the excitation dynamics is determined by a set of linear equations:

$$[\omega_{\text{SP}i}^2 - \omega^2 - i\eta_i\omega] \vec{P}_i = \frac{1}{3}r_i^3\omega_{\text{P}i}^2 4\pi\epsilon_0 \left[\vec{E}_i^{(ext)} + \sum_{j \neq i}^N \vec{E}_{j,i}(\vec{P}_j, \vec{d}_{j,i}, k) \right]. \quad (1)$$

Here, \vec{P} , r , ω_{P} , ω_{SP} and η correspond to the dipole moment, radius, bulk and surface plasmon frequencies, and

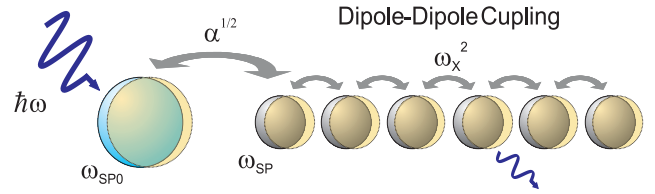


FIG. 1. (Color online) - An external source ($\hbar\omega$) excites the surface plasmon ($\omega_{\text{SP}0}$) of a NP which has an effective coupling ($\alpha^{1/2}\omega_x^2$) to a linear array of NPs where detection takes place.

electronic damping of the i^{th} NP. ϵ_0 is the free space permittivity. $\vec{E}_i^{(ext)}$ and $\vec{E}_{j,i}$ are respectively the external field and the electric field produced by the j^{th} NP at the i^{th} NP. In general, $\vec{E}_{j,i}$ is a complex function that depends on the separation \vec{d} between NPs and the wave vector \vec{k} . However, if $|d|$ is small, $\vec{E}_{j,i}$ can be evaluated in the near field approximation:

$$\vec{E}(\vec{P}, \vec{d}, k) \stackrel{kd \rightarrow 0}{\approx} \frac{\vec{P} - 3\hat{d}(\vec{P} \cdot \hat{d})}{4\pi\epsilon_0 n^2 d^3}, \quad (2)$$

where n is the refractive index of the host material.

For a linear array of NPs, plasmon oscillations can only be transverse (T) or longitudinal (L) to the chain axis, and due to the cubic dependence of E on d , it is a good approximation to neglect contributions beyond first neighbors [2]. Therefore, a matrix form of Eq. 1 reads:

$$(\mathbb{I}\omega^2 - \mathbb{M}) \mathbf{P} = \mathbb{R}\mathbf{E} \quad (3)$$

where \mathbb{M} is tridiagonal, with $M_{i,i}$ given by $\tilde{\omega}_{\text{SP}0}^2 = \omega_{\text{SP}0}^2 - i\eta_0\omega$ for $i = 0$ (the LE-NP) and $\tilde{\omega}_{\text{SP}}^2 = \omega_{\text{SP}}^2 - i\eta\omega$ for $i \neq 0$ (i.e. any of the equidistant identical NPs along the chain). The $M_{i,j}$ are $\omega_{\text{X},i,j}^2 = \frac{\gamma^{T,L}\omega_{\text{P}i}^2}{3n^2} \left(\frac{r_i}{d_{i,j}}\right)^3$, with $\gamma^T = 1$ and $\gamma^L = -2$. \mathbb{R} is diagonal with $R_{i,i} = -4/3\pi r_i^3 \omega_{\text{P}i}^2 \epsilon_0$.

This description is accurate under the following conditions: 1) system length scales smaller than the wave vector ($kd \ll 1$), and 2) a small ratio between the radius and the interparticle separation ($r/d \lesssim 1/3$) where higher order multipoles are negligible [8]. These conditions result in small r 's and allow us to ignore radiation damping corrections [6].

Excitation dynamics between the different sites i and j is determined by the corresponding matrix elements of the Green's function (GF),

$$\mathbb{D} = (\mathbb{I}\omega^2 - \mathbb{M})^{-1} \mathbb{R}. \quad (4)$$

Since \mathbb{M} is tridiagonal, $D_{ij}(\omega^2)$ admits exact analytical expressions which, for finite systems, show a set of isolated poles at the eigenvalues of \mathbb{M} [9]. As the external source is focused on LE-NP ($i = 0$), the relevant quantity is

$$D_{00} = \frac{-\frac{4}{3}\pi r_0^3 \omega_{\text{P}0}^2 \epsilon_0}{[\omega^2 - \tilde{\omega}_{\text{SP}0}^2] - \alpha \Pi(\omega)}, \quad (5)$$

with $\text{Im} D_{00}(\omega)$ giving a local density of plasmonic states (LDPS). Here $\alpha^{1/2} = \omega_{\text{X}0,1} \omega_{\text{X}1,0} / \omega_{\text{X}}^2$ represents a relative effective coupling strength ($\alpha = 0$ describes an isolated LE-NP), while $\alpha \Pi(\omega)$ is a "self-energy" function accounting for the presence of the linear array. For an ordered semi-infinite system, \mathbb{M} acquires a continuous spectrum and $\Pi(\omega)$ satisfies a quadratic Dyson equation [9]. Only one of its two solutions is physically correct:

$$\Pi(\omega) = \frac{1}{2} [\omega^2 - \tilde{\omega}_{\text{SP}}^2] - \text{sgn}(\omega^2 - \omega_{\text{SP}}^2) \frac{1}{2} \sqrt{[\omega^2 - \tilde{\omega}_{\text{SP}}^2]^2 - 4\omega_{\text{X}}^4}. \quad (6)$$

The other one is on a non-physical Riemann sheet that yields a state that would grow in time. $\text{Im} \Pi(\omega)$ accounts not only for excitation decay through electronic damping η but also for its escape through the waveguide. In the weak damping limit (WDL) where $\eta \rightarrow 0$, each frequency component of the excitation propagates with group velocity $\frac{d}{d\omega} \sqrt{4\omega_{\text{X}}^4 - [\omega^2 - \omega_{\text{SP}}^2]^2}$ within the continuous band $|\omega^2 - \omega_{\text{SP}}^2| \leq 2\omega_{\text{X}}^2$, the "passband" [2].

$D_{00}(\omega)$ may have up to four physical poles chosen among:

$$\tilde{\omega}_{\pm}^2 = \frac{[\beta - \alpha(\beta + 1)/2]_{\pm}}{(1 - \alpha)} \pm \frac{\alpha}{2(1 - \alpha)} \sqrt{(1 - \beta)^2 - 4V^2(1 - \alpha)}, \quad (7)$$

where $\tilde{\omega}_{\pm}^2 = \frac{\omega_{\pm}^2}{\omega_{\text{SP}}^2}$, $\beta = \frac{\tilde{\omega}_{\text{SP}0}^2}{\omega_{\text{SP}}^2}$, and $V = \frac{\omega_{\text{X}}^2}{\omega_{\text{SP}}^2}$. The physical analysis of the poles is simplified in the WDL. The mapping to a quantum tight-binding system is direct and we may benefit from recent results [10]. For such systems, poles with a negative imaginary part correspond

to *resonances* in the response function. If the poles are real, they should be in the physical Riemann sheet of the self-energy to correspond to *localized* states. The use of Π in the non-physical Riemann sheet, may also lead to real poles $\tilde{\omega}_{\pm}^2$. Since they do not correspond to actual plasmonic eigenmodes nor to resonances, they are called *virtual* states [10, 11]. However, we will see that their influence on the LDPS within the passband is as strong as that of the physical localized states. The continuous line in Fig. 2 shows the two positive poles, $\tilde{\omega}_{\pm} = +\sqrt{\tilde{\omega}_{\pm}^2}$, as function of $\alpha^{1/2}$, a variable that increases for diminishing separation between the LE-NP and the waveguide. A

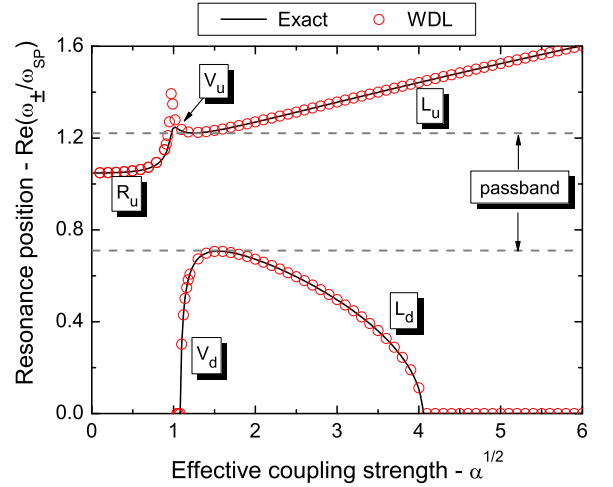


FIG. 2. Real part of ω_{\pm} , the GF's poles, as function of $\alpha^{1/2}$. Here, $\omega_{\text{SP}0}^2 / \omega_{\text{SP}}^2 = 1.1$, $\eta = 0.5\omega_{\text{SP}}$, $\eta_0 = \omega_{\text{SP}}$, and $\omega_{\text{X}}^2 / \omega_{\text{SP}}^2 = 0.25$. **L**, **V**, and **R** stand for *localized*, *virtual* or *resonant* state. Subscript **up** and **down** stand for the position of $\text{Re}(\omega_{\pm})$ relative to ω_{SP} .

quantity of experimental interest is the square dipole moment of the N^{th} NP, $|P_N|^2$, produced when the LE-NP is externally excited with an electric field E_0 .

$$|P_N|^2 = |D_{N0}|^2 |E_0|^2 \quad (8)$$

The elements of a finite $\mathbb{D}(\omega)$ satisfy simple relationships [12] which, extended to an infinite case, enabled us to find the response of our system at an arbitrary position N given an excitation at position $i = 0$:

$$D_{N0}(\omega) = D_{00}(\omega) \alpha_{1-0}^{1/2} e^{-N/\xi(\omega)}, \quad (9)$$

where $\alpha_{1-0}^{1/2} = \omega_{\text{X}1,0}^2 / \omega_{\text{X}}^2$ and $\xi^{-1}(\omega) = \ln(\omega_{\text{X}}^2 / \Pi) = \kappa \pm ik$. In the WDL, excitations within the passband propagate with wave number k , while those outside the passband decay with κ , an inverse localization length. The inclusion of electronic damping adds a further decay and smears out the dispersion relation. This overall behavior

is consistent with the numerical solutions including full retardation effects under similar conditions [7].

The exact calculation of ω_{\pm} , shown in Fig. 2, requires an iterative procedure as β , V and $\tilde{\omega}_{\pm}$ depend on ω . However, the WDL enables us to solve Eq. 7 up to a good approximation (see Fig. 2), finding the critical parameters that describe transition among the different regimes. As α increases from zero, at

$$\alpha_{c1} = \frac{2\beta + 4V^2 - \beta^2 - 1}{4V^2}, \quad (10)$$

$\text{Im}(\tilde{\omega}_{\pm})$ becomes zero, defining the transition between resonant and virtual states. A further increase of α to $\alpha_{c2(-)}$,

$$\alpha_{c2(+/-)} = 2 \pm \frac{(1 - \beta)}{V}, \quad (11)$$

results on $\text{Re}(\tilde{\omega}_{\pm}^2) = 1 \pm 2V$, i.e. the pole touches the edge of the passband, indicating the transition between virtual and localized states. For small α there is a non-physical pole with $\text{Im}(\tilde{\omega}_{\pm}) > 0$ which at $\alpha = \alpha_{c3(-)}$ ($\alpha = 1$ for $\beta < 1$), with

$$\alpha_{c3(+/-)} = \frac{\beta}{V^2} \frac{1 \pm \sqrt{1 - 4V^2}}{2}, \quad (12)$$

becomes real but falls on a non-physical Riemann sheet, indicating the appearance of a virtual state that only becomes a physical localized state at $\alpha_{c2(+)}$ and vanishes again at $\alpha_{c3(+)}$.

In the resonant states regime, the real part of this pole lies within the passband ensuring the energy transfer to the waveguide. Following the same reasoning, it is clear that spectra with localized states, isolated physical poles placed outside the passband, yield poor excitation transfer. The exception occurs when those poles are close to the band edges as compared with their natural width η . In such a case, the overlap between the LDPS and the passband enables excitation transfer. The case of virtual states is particularly interesting: Even when they are not physical poles, they have a non-trivial effect on the LDPS, and hence in D_{N0} . In both, virtual and localized regimes, the LDPS is roughly modulated by a factor $1/(\omega^2 - \omega_{\pm}^2)$. This ensures the singular accumulation of continuum states at the band edge necessary to nucleate the localized state. Hence, at the virtual-localized critical point the LDPS presents a maximum that strongly favors the excitation transfer. Fig. 3 shows the excitation transfer as a function of ω^2/ω_{SP}^2 for different NP sites along the chain. Two parameter sets are enough to illustrate the typical behavior discussed above: Fig. 3-A shows a resonant state, while Fig. 3-B shows a virtual and a localized state.

Fig 4 shows the maximum excitation transfer, $|P_N|^2$, enabled by a variation of ω at each system configuration.

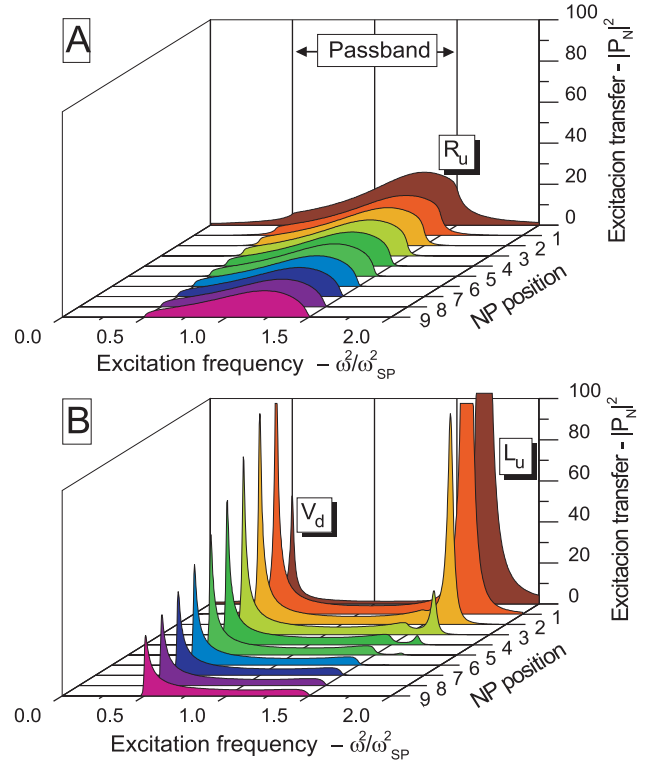


FIG. 3. (Color online) Square dipolar moment (in arbitrary units) as function of the NP position along the chain and excitation frequency. Here, $\eta = 0.01\omega_{SP}$, $\eta_0 = 0.02\omega_{SP}$, and $\omega_x^2/\omega_{SP}^2 = 0.25$. In **Fig. A** $\alpha^{1/2} = 0.9$, $\omega_{SP0}^2/\omega_{SP}^2 = 1.1$ and in **Fig. B** $\alpha^{1/2} = 1.8$, $\omega_{SP0}^2/\omega_{SP}^2 = 1.3$. **L**, **V**, and **R** stand for localized, virtual or resonant states.

Superposed are the critical values resulting from Eqs.10-12. Consistently with the above discussion, an appreciable transfer occurs in the resonant state regime. However, the maximum appears at the transition between virtual and localized states. Note that the optimal configuration for excitation transfer does not occur for $\omega_{SP0} = \omega_{SP}$ and $\alpha = 1$, where the LE-NP is indistinguishable from the others, as one might naïvely expect. Instead, it occurs for the highly asymmetric configuration where a virtual-localized transition appears.

Another counter-intuitive result is that a high transfer efficiency could be achieved even if ω_{SP0} and ω_{SP} are arbitrarily different so ω_{SP0} gives a localized state outside the passband. In analogy with the addatom in an Anderson-Newns model [10], a strong interaction with the substrate captures a state from the continuum spectrum to build a second localized state that would constitute the “anti-bonding” orbital of a dimer [13]. This occurs through a virtual-localized transition and thus leads to the optimal excitation transfer shown in Fig 4. Experimentally, these critical points could be achieved by properly tuning the distances, sizes, shapes and materials of the system. Additionally, this configuration acts as a very narrow filter

for the external frequency in resonance with the passband edge (See Fig. 3-B), where small group velocity also favors excitation build-up. The control of this critical phenomenon opens up many possibilities for applications.

Finally, we note that the excitation transfer can change various orders of magnitude as d_0 is slightly changed. This occurs because α varies with d_0^{-6} and, depending on the value of β , the system response sweeps through different regimes within a narrow interval of α . The extreme sensibility of excitation transfer on distances enables a new form of plasmon ruler suitable for biological and chemical applications [14]. Similarly, as small changes on the refractive index modify dramatically the coupling ω_X^2 and hence the passband, the excitation transfer is also extremely sensitive to the dielectric environment for a system tuned at the virtual-localized transition.

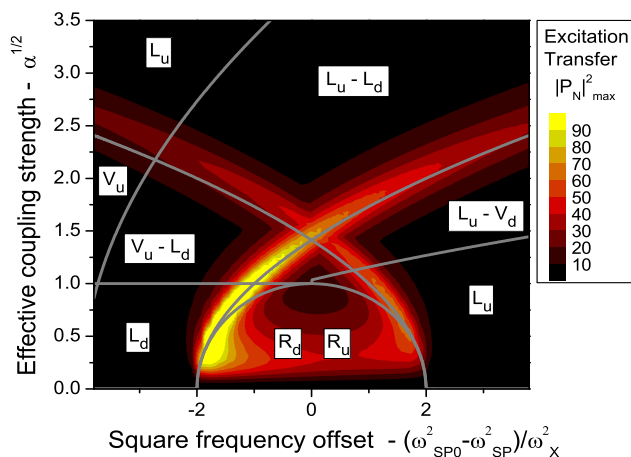


FIG. 4. (Color online) Color scale shows the maximum excitation transfer to the 5th NP ($\max |P_5(\omega)|^2$ in arbitrary units) for realistic values $\eta = 0.01\omega_{SP}$ and $\eta_0 = 0.02\omega_{SP}$. The continuous lines show the critical parameters in the WDL. **L**, **V**, and **R** indicate the existence of *localized*, *virtual* or *resonant* states.

In summary, we have demonstrated that a linear array of NPs is a versatile tool to address different regimes of plasmonic excitation transfer. The richness of the excitation spectrum is so vast that it could not be explored by a mere empirical or numerical experimentation, but requires of a deep understanding of the parametric phase space. We have shown that small variation of parameters (e.g. distances, dielectric media, sizes and shapes) can sweep the excitation spectrum from normal resonances to various forms of localized states, passing through the non-trivial spectra associated with the presence of virtual states. With these considerations we have suggested a broad range of applications. Besides, as all the analysis has been made in terms of adimensional parameters,

our conclusions are completely general. Particularly the phase diagram of Fig. 4 is universal and applicable to any of the broad class of systems represented as linear arrays of damped oscillators [15].

The authors acknowledge the financial support from CONICET, ANPCyT, MinCyT-Córdoba and SeCyT-UNC. Bustos-Marín acknowledges Axel Dente for useful discussions.

-
- [1] S. A. Maier, *Plasmonics: Fundamentals and Applications* (Springer Press, New York, 2007); L. Novotny and B. Hecht, *Principles of Nano-Optics* (Cambridge. Press, Cambridge, 2007).
 - [2] M. L. Brongersma, J. W. Hartman, and H. A. Atwater, *Phys. Rev. B* **62**, R16356 (2000).
 - [3] L. Burin, H. Cao, G.C. Schatz, and M.A. Ratner, *J. Opt. Soc. Am. B* **21**, 121 (2004); M. Guillon, *Opt. Express* **14**, 3045 (2006); S. Zou and G. C. Schatz, *Nanotechnology* **17**, 2813 (2006); E.M. Perassi, L.R. Canali and E.A. Coronado, *J. Phys. Chem. C* **113**, 6315 (2009); E.R. Encina, E.M Perassi, E.A. Coronado, *J. Phys. Chem. A* **113**, 4489 (2009).
 - [4] S. A. Maier, *et al.*, *Nature Mater.* **2**, 229 (2003); M.I. Stockman, S. V. Faleev, and D. J. Bergman, *Phys. Rev. Lett.* **88**, 067402 (2002); M. I. Stockman, *Phys. Rev. Lett.* **93**, 137404 (2004).
 - [5] D. S. Citrin, *Nano Lett.* **4**, 1561 (2004); A. Alù and N. Engheta, *Phys. Rev. B* **74**, 205436 (2006).
 - [6] A. V. Malyshev, V. A. Malyshev, and J. Knoester, *Nano Lett.* **8**, 2369 (2008); J. V. Hernández, L.D. Noordam, and F. Bobicheaux, *J. Phys. Chem. B* **109**, 15808 (2005); T. D. Backes and D. S. Citrin, *Phys. Rev. B* **78**, 153407 (2008).
 - [7] V. A. Markel and A. K. Sarychev, *Phys. Rev. B* **75**, 085426 (2007).
 - [8] S. Y. Park, D. Stroud, *Phys. Rev. B* **69**, 125418 (2004).
 - [9] H.M. Pastawski and E. Medina, *Rev. Mex. Fis.* **47s1**, 1 (2001) and references therein; E. N. Economou, *Green's Functions in Quantum Physics*, 3rd ed. (Springer, Heidelberg, 2006).
 - [10] A. D. Dente, R.A. Bustos-Marín, and H.M. Pastawski, *Phys. Rev. A* **78**, 062116 (2008).
 - [11] H. Hogeve, *Phys. Lett. A* **201**, 111 (1995); P. Serra, S. Kais and N. Moiseyev, *Phys. Rev. A* **64**, 062502 (2001); A. M. Pupasov, B. F. Samsonov and J.-M. Sparenberg, *Phys. Rev. A* **77**, 012724 (2008).
 - [12] D. J. Thouless, *J. Phys. C* **5**, 77 (1972); H. M. Pastawski, J. F. Weisz and S. Albornoz, *Phys. Rev. B* **28**, 6896 (1983); E. Kilic, *Appl. Math. and Comput.* **197**, 345 (2008).
 - [13] P. Nordlander *et al.*, *Nanolett.* **4**, 899 (2004).
 - [14] G. L. Liu, *et al.*, *Nature Nanotech.* **1**, 47 (2006).
 - [15] L. A. Sweatlock, S. A. Maier, H. A. Atwater, *Proceedings - Electronic Components and Technology Conference*, 1648 (2003); H.L. Calvo, E. P. Danieli, H. M. Pastawski, *Phys. B* **398**, 317 (2007); L. Gutiérrez *et al.*, *Phys. Rev. Lett.* **97**, 114301 (2006)